Utilizing the right phosphor in near-ultraviolet and blue light-emitting diode devices to generate white illumination

Dieu An Nguyen Thi[1], Nguyen Doan Quoc Anh[2], Phan Xuan Le[3]
[1]Faculty of Electrical Engineering Technology, Industrial University of Ho Chi Minh City, Ho Chi Minh City, Viet Nam
[2]Faculty of Electrial and Electronics Engineering, Ton Duc Thang University, Ho Chi Minh City, Vietnam
[3]Faculty of Mechanical-Electrical and Computer Engineering, School of Engineering and Technology, Van Lang University, Ho Chi Minh City, Vietnam

Article Info

Article history:

Received Nov 30, 2021
Revised Jun 4, 2022
Accepted Jun 20, 2022

Keywords:

Color homogeneity
Luminous flux
Monte Carlo theory
Solid-state lighting
White light emitting diodes

ABSTRACT

In the scenario of solid-state lighting (SSL) gradually replacing old standard techniques; the pc-LEDs (or diodes based on conversion phosphor) becomes a common method for creating white illumination, based on SSL. As of now, both of the UV-LEDs and the blue LEDs have been still being considered for the task of creating white illumination through phosphor excitation as it hasn't been known which LED type is truly superior. It is common that when it comes to phosphor, people will overlook the performance in LED devices with a wavelength range of 365 nm to 470 nm. Our research demonstrates the information concerning extrinsic quantum efficacy in the InxGa1-xN LED devices with the mentioned range as well as combines the information and the effectiveness of phosphor for the task of examining the performance of near-UV and blue LEDs and creating white illumination. In addition, the research demonstrates recreations for the task of assessing the white illumination mixtures under the correlated color temperature of 3000 K and 4000 K in the two LED structures.

Corresponding Author:

Phan Xuan Le
Faculty of Mechanical-Electrical and Computer Engineering, School of Engineering and Technology
Van Lang University
Ho Chi Minh City, Vietnam
Email: le.px@vlu.edu.vn

1. INTRODUCTION

As of today, the optical field appears to undergo significant changes, as the LED devices become increasingly more common as a way to create white illumination, substituting for the old standard optical devices such as incandescent and fluorescent [1]-[3]. The LED device involves two procedures. The first involves mixing the LED devices with red, green, blue and occasionally yellow, which can be called RGB or RGBA (with yellow LED). The second involves utilizing phosphor transmutation with a color created via a down-conversion phosphor under the excitation of an LED pump. The enhancement of the LED performance for the spectrum's green zone was known, but the performance of the green as well as yellow LED devices may not be comparable to the that of the ones based on conversion phosphor [4], [5]. For this reason, the white light emitting diode (WLED) devices (or white LEDs) made by the industry would be mostly pc-WLED devices (or LED devices based on conversion phosphor) which may account for over seventy five percent of the LED devices made for the market. We have two ways to create white illumination using the pc-LED devices. The first way involves exciting at least a phosphor of the spectrum's green-to-red zone. For certain instances, we should utilize a direct-generating LED for the spectrum's red zone. This, however, will not be covered by our research. The second way involves exciting the phosphors via a near-UV LED to create illumination for the observable spectrum [6]-[8].

Taking the ISO standard into account, the near-UV zone has a wavelength limit of 300–400 nm. This research, however, will count the LED devices with a limit of 365-420 nm as near-UV LED for the purpose of differentiate between the said LED and the LED under roughly 450 nm wavelength. Utilizing the near-UV LED, however, raises the Stoke loss needed for the creation of white illumination [9], [10]. Suppose the LED devices and the phosphors employed in both ways offer similar performances, the near-UV way would suffer a penalty of roughly 7% to 23%, based on the proportions between 450 nm and 420 nm as well as 450 nm and 365 nm. On the other hand, both the LED devices and the phosphors would not offer one-hundred-precent intrinsic quantum efficacy. As such, if we need the near-UV way to become as effective as the blue LED way, the near-UV LED's performance must solve such discrepancy, or the phosphors of the near-UV LED must offer better performance than the blue LED, or the near-UV LED must offer certain benefits [11], [12].

In order to utilize the near-UV in the pc-LED devices for the creation of white illumination, we must have a blue phosphor, whereas the blue LED devices offer blue element in the white illumination. At the start of the SSL thrust, with the better ability to select the blue element in the white illumination from the near-UV LED devices, the optical creators would be able to acquire superior color rendering index (CRI) for a specific color point, which resembles the fluorescence with a phosphor structure of three bands employed for creating the white illumination that offers significant performance as well as CRI. However, the near-UV LED's emission would be quite similar to the needed blue emission in a phosphor, which introduces some obstacles for the development of desirable phosphors with significant performance. Our research examines such obstacles along with the disadvantages found in the LED devices.

2. LED CONSIDERATIONS FOR SOLID STATE LIGHTING

The $In_xGa_{1-x}N$ structure would be the foundation for the lighting quantum wells utilized in the near-UV as well as the blue LED devices. It is possible to adjust the bandgap among the end members from 3.4 eV at about 365 nm wavelength in GaN[5] to 0.7 eV at about 1771 nm wavelength in InN. If the task is shifting the bandgap closer to the UV, we have to utilize the $Al_xGa_{1-x}N$ or $(Al,In)_xGa_{1-x}N$ structures. However, the performances offered by these LED devices appear to be rather inferior[7] and would not be possible ways to create the white illumination. Many $In_xGa_{1-x}N$ LED versions are available thanks to various epitaxial growth methods, substrates, structures of the chip, the form of packaging, and optical separation techniques. The research shall focus on the thin film form of LED. The LED forms and producers may lead to certain distinctions, but the universal trends could be relevant to $In_xGa_{1-x}N$ [13], [14].

In Figure 1(a), we can see the extrinsic quantum efficacy (or η_{ex}) with the peak wavelength of a set of near-UV and blue LEDs under the current density (or *J*) measured at 35 A/cm^2. The highest η_{ex} value is achieved when the wavelength is 425 nm. On the basis of the η_{ex} alteration with wavelength under 35 A/cm^2 as well as η_{ex} being the superior limit of energy performance, the energy performance in the near-UV LEDs would not receive any benefit under the wavelengths less than roughly 405 nm with the blue LEDs emission under the wavelength ranging from 440 to 450 nm, which is the common option for white illumination. Such $In_xGa_{1-x}N$ LED activity indicates that the phosphors excitable under wavelengths less than 405 nm would barely have a practical use for white illumination with high need for performance [15], [16].

The η_{ex} displays a sharp fall as it is shifted closer to the UV. On the other hand, when it is enhanced to fit the zone of smaller wavelength, η_{ex} could reach forty five percent under the peak wavelength of 365 nm. Despite the significant dislocation density in $In_xGa_{1-x}N$ advancing from 10^8 cm^{-2} to 10^9 cm^{-2}, the higher quantum efficacy as well as the higher concentration of indium would attract substantial attention for theories and is considered to resulted from spinodal decay which is linked to the InN-GaN alloys.[10] The small η_{ex} value for both pure GaN and AlGaN may be partially caused by the lack of variation linked to the spinodal decay. Furthermore, the absorption of the epistack, notably of the GaN treated with p, as well as the reduction in the reflection in the mirror employed in the thin-film structure would be the main cause of the η_{ex} decrease. In addition, the quantum efficacy decreases when shifting closer to the green peak under the wavelength of 425 nm, while yielding a performance ten percent lower under the wavelength of 450 nm. Beside the alteration in the LED's extrinsic efficacy, the Stoke loss of the down-converison can have an influence on the pc-LED's energy efficacy. When it comes to the blue LEDs, the blue element in white radiation comes from the LED device. Meanwhile in the near-UV LED, the LED emission would be unsuitable for the blue element in the white illumination. Being the primary interest for tailoring illumination with high energy efficacy, the luminous flux rises under greater wavelength till the peak wavelength reaches 555 nm. Meanwhile, the blue stimulus function controlling the chromatic coordinates achieves the highest value within the blue zone under the wavelength of roughly 445 nm. As such, we must select an option for the blue peak to achieve desirable performance, color point as well as chromatic output. In the case of the blue LEDs, the common option to yield the blue element would be a wavelength peaking at roughly 440 nm. As this research examines the energy efficacy in the illumination through the near-UV LEDs as well as the blue LEDs, the relative efficacy would be determined by the scaled extrinsic efficacy in (1) [17], [18].

$$\eta eff(\lambda) = \eta ex \frac{\lambda}{440} \tag{1}$$

As displayed by Figure 1, η_{eff} would be a wavelength function as well. η_{eff} would be identical to η_{ex} under the shown wavelength. Within the zone of smaller wavelength, the efficacy suffers a fall, which is caused by the necessary transmutation turning the near-UV photons into blue photons, if the transmutation efficacy reaches one hundred percent. η_{eff}, therefore, would be the superior limit for energy efficacy in near-UV LEDs. Such alteration changes the optimal peak wavelength to 431 nm. Such event happens under the wavelength of 395 nm with the discrepancy being five percent. It is necessary to consider such result when we assess the near-UV LEDs' efficiency under greater currents which makes them superior to the blue LEDs. The altered efficacies under the wavelengths of 425 nm and 440 nm would be almost identical, which means that the most desirable wavelength range would be 420-400 nm. It is possible to advance from 425 nm to 440 nm by utilizing a phosphor. The quantum efficacy would be then under one hundred percent. As such, with the value of 35 A/cm^2, it would be more appropriate to choose the blue LEDs. Figure 1 displays the necessary η_{ex}, being equal to η_{ex} under the wavelength of 440 nm, which is determined by formula 2, with ηex_440 nm being the extrinsic quantum efficacy in the blue LED under the peak wavelength measured at 400 nm [19]-[21].

$$\eta ex\_eq(\lambda) = \eta ex\_440\, nm \frac{440}{\lambda} \tag{2}$$

Some instances of LEDs within the violet zone exist, such as 410 nm or 415 nm, along with the extrinsic quantum efficacies over the parity line shown by Figure 1. However, it proves to be more difficult when shifting to smaller wavelengths. In addition, searching for a blue phosphor that offers significant absorption coefficient as well as quantum efficacy is a fairly difficult task.

The optical field tends to opt for greater drive currents to lower the cost [22], [23]. With greater current, the near-UV chips may offer benefits, which is demonstrated by Figure 2. The Figure demonstrates the η_{ex} alteration, which is a function for the current density of the LED emission in the wavelength range of 390 nm to 460 nm. Regarding every wavelength, the extrinsic quantum efficacy rises when the current is raised from extremely small current densities to highest values under the range of 1 A/cm^2 to 10 A/cm^2. Raising the drive current even more will lead to lower efficacy 14. The fall will be worsened if the peak wavelength is raised. The decrease in the inner quantum efficacy under significant current densities would be a droop effect mainly caused by the non-radiative Auger recombination 15. Taking the respective emission measured at 440 nm into account, the intersection happens when the values are 350 A/cm^2, 71 A/cm^2, 20 A/cm^2, 1.5 A/cm^2 with respective peak wavelengths of 390 nm, 400 nm, 420 nm, 460 nm. In Figure 2, we can see the information regarding η_{eff} and J, as well as the peak wavelength of 440 nm in the formula 1. Having such alteration, the peak wavelength of 420 nm would be the best choice when current densities exceed 50 A/cm^2 between the peak wavelengths. In the case of current densities from 5 A/cm^2 to 50 A/cm^2, the best peak wavelength would be 440 nm for the LED devices chosen. When it comes to smaller current densities, the best wavelength would be 460 nm. In order to generate effective illuminations, we would have to take into account choosing the most desirable near-UV LED under significant current as well as the energy efficacy under smaller current. When high current is necessary, the energy efficacy would suffer from a penalty, making the heat control more complex for the LED structure. This would require a new material used for heat control and for limiting the deterioration. We need to carefully examine such aspects so that we can determine the accurate costs of greater current on the basis of near-UV LED devices.

3. RESULTS AND ANALYSIS

The correlation between the contents of SSL and $YAG:Ce^{3+}$ can be in Figure 1. The results suggest that the purpose of the correlation is sustaining the median CCT values as well as influencing the absorbtivity as well as dispersion for the pair of phosphor sheets in the WLED device. Hence, there may be impact on the hue output as well as lumen for the device, pointing out that the hue output of the device is reliant on SSL concentration. In case said concentration is boosted (2%-20%), the concentration of $YAG:Ce^{3+}$ will decline so that the median values of CCT can be sustained. Similar outcome will occur in the case of WLED devices under a limit between 5600 K and 8500 K.

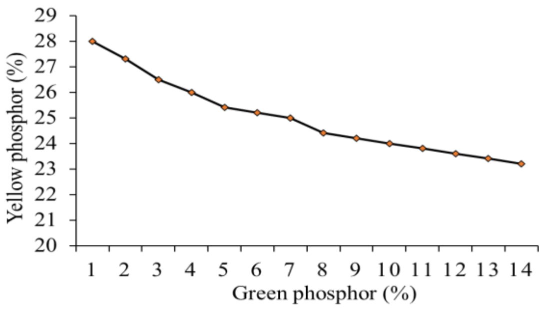

Figure 1. Changing the concentration of phosphor to preserve the average CCT

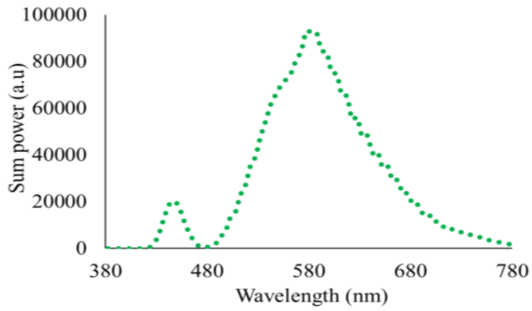

Figure 2. The emission spectra of 3000 K WLEDs as a function of SSL concentration

Figure 2 demonstrates how the concentration of SSL has the ability to alter the transmitting spectrum for the WLED device. The five statistics shown exhibit the spectrum under 3,000 K CCT value. Coming up with an appropriate choice of concentration requires taking the demands of production into account [24]. There are WLED devices that offer considerable hue output, leading to a minimally-reduced lumen. A merge that creates a zone of spectrum will yield white illumination, which is illustrated by Figure 2. Judging two optical spectrum areas between 420 nm and 480 nm as well as 500 nm and 640, it seems that a boost in SSL content will lead to greater intensities. The presence of greater discharge spectrum signifies superior luminous flux. On the other hand, the blue illumination's dispersion for the WLED device appears to be more potent, which may lead to the phosphor sheet as well as the WLED device experiencing more active dispersion. Such an outcome will subsequently augment the hue consistency, a crucial condition in employing SSL [25]. It will not be simple when the task is to manage said consistency for a phosphor layout under huge temperatures. The assessment done by our team has demonstrated the SSL effectiveness under temperatures of 8,500 K as well as 5,600 K for the task of augmenting the hue output for WLED devices.

Our assessment gauged the performance of lumen for the remote phosphor layout with two sheets. With SSL content reaching 20% wt when it starts at 2%, the lumen undergoes considerable surge, which is illustrated by Figure 3. Judging Figure 4, under median values of CCT, the hue aberration suffered from a noticeable penalty as the SSL content declined. The absorptivity in the layer of phosphor might be the cause of this result. The granules of blue phosphor convert the blue light into green light as the said phosphor absorbs the the LED chip's blue illumination. Besides the blue light mentioned, the yellow illumination will be absorbed by the granules in SSL as well. The characteristics of the phosphor yields superior effectiveness for the chip's blue illumination arsorptivity. Hence, if we insert SSL, the green presence in the WLED device will be greater. Hue consistency would be among the most crucial factors of WLED devices. This consistency will influence the cost of the devices. The low cost of SSL might lead to practical uses in large scale.

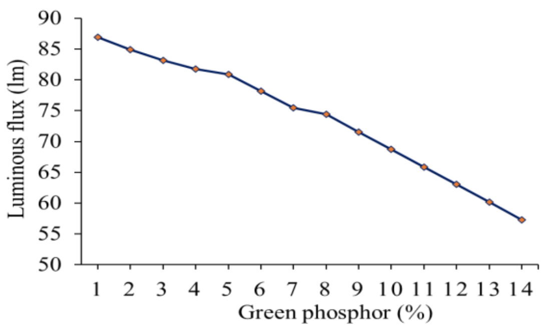

Figure 3. The luminous flux of WLEDs as a function of SSL concentration

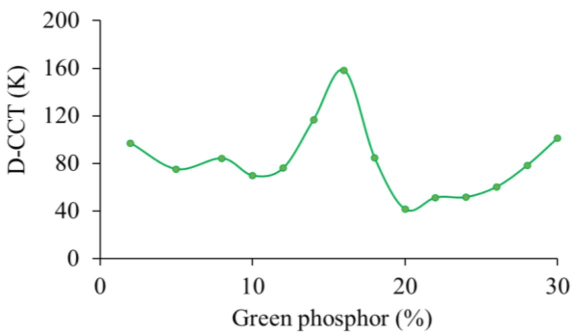

Figure 4. The color deviation of WLEDs as a function of SSL concentration

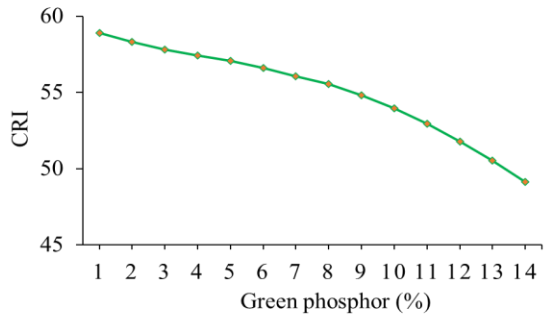

Figure 5. The color rendering index of WLEDs as a function of SSL concentration

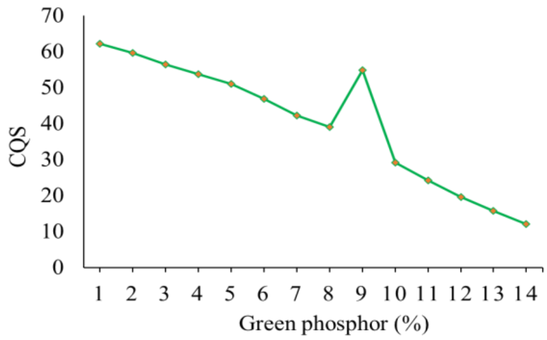

Figure 6. The color quality scale of WLEDs as a function of SSL concentration

Hue consistency is a typical factor responsible for assessing the hue quality in WLED devices. On the other hand, the hue quality is only partially reliant on this factor. Older investigations came up with another factor that can assess hue creation as well as hue output. CRI can determine the authentic hue in an entity when it is illuminated. The lack of chromatic homogeneity is the result of the immoderate content of green illumination compared to the main hues, which are blue, yellow, as well as green. Such an event may alter hue output in the WLED device, subsequently deteriorating the hue consistency. By inserting an SSL sheet, the value of CRI undergoes an insignificant penalty, which is illustrated by Figure 5. It is worth noting that this penalty is unremarkable. It is necessary to focus on acquiring desirable values of CQS. This essential factor would be assessed by CRI, the bias of observers as well as hue coordinates, making it highly useful for gauging hue output [26], [27]. Figue 6 illustrates CQS undergoing a surge due to the existence of a SSL sheet. In case the content of SSL surges while remaining beneath 10% wt, said factor would undergo very little alterations. In the case of 10% wt or higher, the waste of hue caused by green hue's dominance will lead to substantial deterioration for CRI, along with CQS. For this reason, employing SSL requires pinpointing the most suitable concentration for the phosphor.

4. CONCLUSION

Much like the phosphors utilized for the small pressure mercury discharge technique, the energy efficacy would be the primary aspect of the SSL phosphor's creation. For the fluorescent light, the phosphor's activity would be commonly examined by its reaction to radiation at 254 nm as well as 185 nm of the mercury discharge. On the contrary, the $In_xGa_{1-x}N$ LED devices provide a broad spectrum with excitation radiation in the range of 365 nm to green wavelengths, having different efficacies based on the concentration of indium. As such, a phosphor excitable in the wavelength range of roughly 365 nm to roughly 470 nm is commonly considered to be a good choice to be utilized with SSL. Such assumption is incorrect as the LED efficacy undergoes a considerable shift from 365 nm to 470 nm, which is shown at the start of the research. Therefore, examinations of phosphors would not be reliable if they ignore the efficacy of the pump LED as well as the effectiveness regarding the LED radiation. The research offers the information regarding the assessment of suitable phosphors used for the thin-film LED devices. The enhancement of chromatic output can become a vital aspect once the energy efficacy is deemed similar to the standard SSL in blue LED devices. We need to first demonstrate that the LPW in the near-UV pc-LED devices is similar to the LPW in the blue pc-LED devices, via the illumination source's efficiency or via mixing the LED efficacy with the phosphor's quantum efficacy under the excitation radiation under a specific current density. If the information regarding the LED source is inaccessible with the second way carried out to prove a phosphor's efficiency, we must seek more data. It is required to employ the phosphor's absorption coefficient, the trigger ions' radiative duration as well as the information of heat abatement for the task of properly assessing a phosphor. In case the absorption coefficient does not meet the requirement, the phosphor's thickness will become too big, unfit for actual employment. In case the radiative duration appears to be long, such as the $4f$ ⇔ 5*d* shift, it is only possible to utilize the structure for small-flux conditions. Potent heat abatement might become disadvantageous.

ACKNOWLEDGEMENTS

This study was financially supported by Van Lang University, Vietnam.

REFERENCES

[1] H. Y. Yu, *et al.*, "Solar spectrum matching with white OLED and monochromatic LEDs," *Applied Optics*, vol. 57, no. 10, pp. 2659-2666, Apr. 2018, doi: 10.1364/AO.57.002659.

[2] N. Anous, T. Ramadan, M. Abdallah, K. Qaraqe, and D. Khalil, "Impact of blue filtering on effective modulation bandwidth and wide-angle operation in white LED-based VLC systems," *OSA Continuum*, vol. 1, no. 3, pp. 910-929, Nov. 2018, doi: 10.1364/OSAC.1.000910.

[3] H. L. Ke, *et al.*, "Lumen degradation analysis of LED lamps based on the subsystem isolation method," *Applied Optics*, vol. 5, no. 4, pp. 849-854, Feb. 2018, doi: 10.1364/AO.57.000849.

[4] Y. Zhou, *et al.*, "Comparison of nonlinear equalizers for high-speed visible light communication utilizing silicon substrate phosphorescent white LED," *Optics Express*, vol. 28, no. 2, pp. 2302-2316, Jan. 2020, doi: 10.1364/OE.383775.

[5] S. Sadeghi, *et al.*, "Quantum dot white LEDs with high luminous efficiency," *Optica*, vol. 5, no. 7, pp. 793-802, Jul. 2018, doi: 10.1364/OPTICA.5.000793.

[6] A. M. Nahavandi, M. Safi, P. Ojaghi, and J. Y. Hardeberg, "LED primary selection algorithms for simulation of CIE standard illuminants," *Optics Express*, vol. 28, no. 23, pp. 34390-34405, Nov. 2020, doi: 10.1364/OE.408754.

[7] M. Talone, and G. Zibordi, "Spatial uniformity of the spectral radiance by white LED-based flat-fields," *OSA Continuum*, vol. 3, no. 9, pp. 2501-2511, Sep. 2020, doi: 10.1364/OSAC.394805.

[8] S. Xu, *et al.*, "Exploration of yellow-emitting phosphors for white LEDs from natural resources," *Applied Optics*, vol. 60, no. 16, pp. 4716-4722, Jun. 2021, doi: 10.1364/AO.424108.

[9] R. Wan, *et al.*, "Nanohole array structured GaN-based white LEDs with improved modulation bandwidth via plasmon resonance and non-radiative energy transfer," *Photonics Research*, vol. 9, no. 7, pp. 1213-1217, Jun. 2021, doi: 10.1364/PRJ.421366.

[10] X. Xi, *et al.*, "Chip-level Ce:GdYAG ceramic phosphors with excellent chromaticity parameters for high-brightness white LED device," *Optics Express*, vol. 29, no. 8, pp. 11938-11946, Apr. 2021, doi: 10.1364/OE.416486.

[11] M. A. Elkarim, M. H. Aly, H. M. AbdelKader, and M. M. Elsherbini, "LED nonlinearity mitigation in LACO-OFDM optical communications based on adaptive predistortion and postdistortion techniques," *Applied Optics*, vol. 60, no. 24, pp. 7279-7289, Aug. 2021, doi: 10.1364/AO.432364.

[12] E. Quesnel, *et al.*, "Experimental and theoretical investigation of 2D nanoplatelet-based conversion layers for color LED microdisplays," *Optics Express*, vol. 29, no. 13, pp. 20498-20513, May. 2021, doi: 10.1364/OE.425907.

[13] M. Seminara, M. Meucci, F. Tarani, C. Riminesi, and J. Catani, "Characterization of a VLC system in real museum scenario using diffusive LED lighting of artworks," *Photonics Research*, vol. 9, no. 4, pp. 548-557, Mar. 2021, doi: 10.1364/PRJ.414394.

[14] Y. P. Chang, *et al.*, "Laser-assisted LED for adaptive-driving-beam headlights employing ultra-reliable single crystal phosphor for autonomous vehicles," *Optics Express*, vol. 29, no. 17, pp. 26466-26473, Aug. 2021, doi: 10.1364/OE.429951.

[15] A. Alexeev, J. P. M. G. Linnartz, K. Arulandu, and X. Deng, "Characterization of dynamic distortion in LED light output for optical wireless communications," *Photonics Research*, vol. 9, no. 6, pp. 916-928, May. 2021, doi: 10.1364/PRJ.416269.

[16] X. Yu, L. Xiang, S. Zhou, N. Pei, and X. Luo, "Effect of refractive index of packaging materials on the light extraction efficiency of COB-LEDs with millilens array," *Applied Optics*, vol. 60, no. 2, pp. 306-311, Jan. 2021, doi: 10.1364/AO.410141.

[17] B. Yu, *et al.*, "Luminous efficacy enhancement for LED lamps using highly reflective quantum dot-based photoluminescent films," *Optics Express*, vol. 29, no. 18, pp. 29007-29020, Aug. 2021, doi: 10.1364/OE.431345.

[18] Q. Xu, B. Zhao, G. Cui, and M. R. Luo, "Testing uniform colour spaces using colour differences of a wide colour gamut," *Optics Express*, vol. 29, no. 5, pp. 7778-7793, Mar. 2021, doi: 10.1364/OE.413985.

[19] M. Safdar, and P. Emmel, "Perceptually uniform cross-gamut mapping between surface colors," *J. Opt. Soc. Am. A*, vol. 38, no. 1, pp. 140-147, Jan. 2021, doi: 10.1364/JOSAA.411618.

[20] P. Liu, *et al.*, "Laser regulation for variable color temperature lighting with low energy consumption by microlens arrays," *Applied Optics*, vol. 60, no. 19, pp. 5652-5661, Jul. 2021, doi: 10.1364/AO.425426.

[21] C. W. Shin, *et al.*, "Diffraction efficiency enhancement and optimization in full-color HOE using the inhibition characteristics of the photopolymer," *Optics Express*, vol. 29, no. 2, pp. 1175-1187, Jan. 2021, doi: 10.1364/OE.413370.

[22] H. Jiang, *et al.*, "Projection optical engine design based on tri-color LEDs and digital light processing technology," *Applied Optics*, vol. 60, no. 23, pp. 6971-6977, Aug. 2021, doi: 10.1364/AO.432355.

[23] Y. Li, *et al.*, "Effects of remote sediment phosphor plates on high power laser-based white light sources," *Optics Express*, vol. 29, no. 15, pp. 24552-24560, Jul. 2021, doi: 10.1364/OE.433581.

[24] A. R. Motschi, et al., "Identification and quantification of fibrotic areas in the human retina using polarization-sensitive OCT," *Biomed. Opt. Express*, vol. 12, no. 7, 4380-4400, Jun. 2021, doi: 10.1364/BOE.426650.

[25] X. Shi, J. Liu, J. Xiao, and J. Han, "Design of a compact waveguide eyeglass with high efficiency by joining freeform surfaces and volume holographic gratings," *J. Opt. Soc. Am. A*, vol. 38, no. 2, pp. A19-A26, Feb. 2021, doi: 10.1364/JOSAA.404280.

[26] L. Li, and M. J. Escuti, "Super achromatic wide-angle quarter-wave plates using multi-twist retarders," *Optics Express*, vol. 29, no. 5, pp. 7464-7478, Mar. 2021, doi: 10.1364/OE.418197

[27] H. Daicho, K. Enomoto, H. Sawa, S. Matsuishi, and H. Hosono, "Improved color uniformity in white light-emitting diodes using newly developed phosphors," *Optics Express*, vol. 26, no. 19, pp. 24784-24791, Sep. 2018, doi: 10.1364/OE.26.024784.

BIOGRAPHIES OF AUTHORS

Dieu An Nguyen Thi received a master of Electrical Engineering, HCMC University of Technology and Education, VietNam. Currently, she is a lecturer at the Faculty of Electrical Engineering Technology, Industrial University of Ho Chi Minh City, Viet Nam. Her research interests are Theoretical Physics and Mathematical Physics. She can be contacted at email: nguyenthidieuan@iuh.edu.vn.

Nguyen Doan Quoc Anh was born in Khanh Hoa province, Vietnam. He has been working at the Faculty of Electrical and Electronics Engineering, Ton Duc Thang University. Quoc Anh received his PhD degree from National Kaohsiung University of Science and Technology, Taiwan in 2014. His research interest is optoelectronics. He can be contacted at email: nguyendoanquocanh@tdtu.edu.vn.

Phan Xuan Le received a Ph.D. in Mechanical and Electrical Engineering from Kunming University of Science and Technology, Kunming city, Yunnan province, China. Currently, He is a lecturer at the Faculty of Engineering, Van Lang University, Ho Chi Minh City, Viet Nam. His research interests are optoelectronics (LED), power transmission and automation equipment. He can be contacted at email: le.px@vlu.edu.vn.